Effect of ADP on the Orientation of Spin-Labeled Myosin Heads in Muscle Fibers: A High-Resolution Study with Deuterated Spin Labels[†]

Piotr G. Fajer,*,‡ Elizabeth A. Fajer, John J. Matta, and David D. Thomas*

Department of Biochemistry, University of Minnesota Medical School, Minneapolis, Minnesota 55455

Received December 11, 1989; Revised Manuscript Received March 19, 1990

ABSTRACT: We have used electron paramagnetic resonance (EPR) to determine the effects of ADP on the orientational distribution of nitroxide spin labels attached to myosin heads in skinned rabbit psoas muscle fibers. To maximize the specificity of labeling, we spin-labeled isolated myosin heads (subfragment 1) on a single reactive thiol (SH_1) and diffused them into unlabeled muscle fibers. To maximize spectral and orientational resolution, we used perdeuterated spin labels, ^2H-MSL and ^2H-IASL, eliminating superhyperfine broadening and thus narrowing the line widths. Two different spin labels were used, with different orientation relative to the myosin head, to ensure that the results are not affected by unfavorable probe orientation. In rigor, a very narrow three-line spectrum was observed for both spin labels, indicating a narrow orientational distribution, as reported previously (Thomas & Cooke, 1980). ADP induced very slight changes in the spectrum, corresponding to very slight (but significant) changes in the orientational distribution. These changes were quantified by a digital analysis of the spectra, using a two-step simplex fitting procedure (Fajer et al., 1990). First, the magnetic tensor values and line widths were determined by fitting the spectrum of a randomly oriented sample. Then the spectrum of oriented fibers was fit to a model by assuming a Gaussian distribution of the tilt angle (θ) and twist angle (ϕ) of the nitroxide principal axes relative to the fiber axis. A single-Gaussian distribution resulted in inadequate fits, but a two-component model gave excellent results. ADP induces a small ($<5°$) rotation of the major components for both spin labels, along with a similarly small increase of disorder about the average positions.

Following the proposal of the "rotating crossbridge" theory (Huxley, 1969), according to which the pivoting action of an actin-attached myosin head causes force generation and filament sliding, much of the work in the muscle field has concentrated on the identification of distinct head orientations of attached heads [reviewed by Cooke (1986) and Thomas (1987)]. Morales and Botts (1979) suggested that each chemical state of the cycle has a different angle of the myosin head with respect to the fiber axis. Thus, the comparison of head orientation in induced chemical states analogous to those present during contraction could provide details needed to understand the mechanochemical coupling of muscular contraction. Following this approach, we have examined previously the orientation and mobility of spin-labeled myosin heads attached to actin, in relaxed fibers at low ionic strength (Fajer et al., 1985) and in the presence of the nucleotide analogue AMPPNP (Fajer et al., 1988), using electron paramagnetic resonance (EPR).[1] Although we have found crossbridge states different from both the beginning of the contractile cycle (relaxation) and the end (rigor), states in which attached heads are mobile and disoriented (low μ, relaxed) or in which one head is attached as in rigor but the other is detached and mobile (AMPPNP), we have yet to define quantitatively the change of orientations associated with more strongly bound heads. An attractive candidate for one of the states (in addition to rigor) is the acto–myosin–ADP ternary complex. The correlation between the maximum shortening velocity and the rate of ADP release in solution (Siemiankowski et al., 1985) or in fibers (Pate & Cooke, 1985) suggests its coupling to force generation. Indeed, the addition of ADP to rigor fibers reduces tension slightly without affecting stiffness (Tanner et al., 1989), suggesting a partial reversal of the power stroke without causing detachment.

Some optical probes attached to myosin heads have been shown to change orientation upon ADP addition. Burghardt et al. (1983) and Borejdo et al. (1982) measured a change of IATR dichroism. More recently, Ajtai and Burghardt (1987) observed a change in IEDANS fluorescence. However, there is little support for a substantial ADP-induced movement of the whole myosin head. Low-angle X-ray diffraction showed no significant change or head orientation as compared to rigor (Rodger & Tregear, 1974) and neither did intrinsic birefringence (Oboriah & Irving, 1989). Also, in our preliminary paper (Thomas et al., 1985) on the effect of ADP on EPR spectra, we detected no significant ($<10°$) reorientation of the maleimide spin-labeled myosin head. In the present study, to increase the angular sensitivity of the EPR spectra, we have used perdeuterated spin labels: maleimide spin label (^2H-MSL) and iodoacetamide spin label (^2H-IASL), which have narrower intrinsic line widths than the corresponding protonated spin labels. We have also applied a newly developed method of EPR spectral analysis (Fajer et al., 1990) to analyze

* To whom correspondence should be addressed.
‡ Present address: Institute of Molecular Biophysics, Florida State University, Tallahassee, FL 32306.

[1] Abbreviations: PADS, peroxylamine disulfonate; KPr, potassium proprionate; SEM, standard error of the mean; EPR, electron paramagnetic resonance; S1, myosin subfragment 1; ^2H-MSL, perdeuterated N-(1-oxy-2,2,6,6-tetramethyl-4-piperidinyl)maleimide; ^2H-IASL, perdeuterated N-(1-oxy-2,2,6,6-tetramethyl-4-piperidinyl)iodoacetamide; AP_5A, P^1,P^5-bis(5'-adenosyl) pentaphosphate.

quantitatively a complex angular distribution of nitroxide labels with high resolution.

METHODS

Sample Preparation. Glycerinated psoas muscle fibers from New Zealand white rabbits were prepared by chemical skinning in 0.5% Triton X-100 and glycerination in 25% glycerol as described in Fajer et al. (1988).[2] The sarcomere length of the fibers was 2.3 ± 0.1 μm as measured by laser diffraction. Subfragment 1 (S1) was prepared from myosin by digestion with α-chymotrypsin and labeled with ^{2}H-MSL (perdeuterated *N*-(1-oxy-2,2,6,6-tetramethyl-4-piperidinyl)maleimide) or with ^{2}H-IASL (perdeuterated *N*-(1-oxy-2,2,6,6-tetramethyl-4-piperidinyl)iodoacetamide) as described for the protonated labels in Fajer et al. (1988). In the case of ^{2}H-IASL the labeling procedure was modified by initially incubating 0.1 mM S1 with 0.065 mM spin label (120 mM KCl, 1 mM EDTA, 10 mM MOPS, 10 mM K_2PP_i, pH 7) for 12 h, followed by 4 h of labeling with an additional 0.065 mM ^{2}H-IASL. For both labels, the extent of labeling was 0.9–1.0 labels/S-1 as determined from double integration of EPR spectra. The extent of labeling was matched by the fractional inhibition of K/EDTA-ATPase, indicating that $94 \pm 5\%$ (^{2}H-MSL) or $99 \pm 5\%$ (^{2}H-IASL) of the spin labels were attached to cysteine 707 (SH1) or to cystein 698 (SH2). The spin labels were a gift from Dr. Al Beth of Vanderbilt University. The details of the sample preparation, labeling, and characterization are given in Fajer et al. (1988). The labeled S1 was infused into muscle fiber bundles while the EPR signal was monitored, and the unbound S1 was washed out with rigor solution. Myofibrils were prepared by homogenization of S1-decorated fibers using a Tekmar tissue homogenizer.

Solutions. The rigor solution consisted of 100 mM potassium propionate (KPr), 2 mM $MgCl_2$, 1 mM EGTA, and 10 mM MOPS, pH 7.0. The ADP solution (4 mM MgADP) had a lower salt concentration (80 mM KPr) to maintain a constant ionic strength of 114 mM. Hexokinase (100 μg/mL) (Sigma) and glucose (10 mM) were added to remove any contaminant ATP, and AP_5A P^1,P^5-bis(5'-adenosyl) pentaphosphate (100 μM) (Boehringer) was added to inhibit myokinase.

Electron Paramagnetic Resonance. Fiber bundles (0.5 mm) were placed in 1-mm glass capillaries and held isometrically by surgical thread tied to the bundle ends. Solutions were continuously flowed over the fibers at a rate of 0.2 mL/min. EPR experiments were performed on a Bruker ER-200D spectrometer (Bruker Spectrospin, Billereca, MA), using a TM_{110} cavity modified to accept a fiber-containing capillary parallel to the static magnetic field (Thomas & Cooke, 1980). The spectra were recorded at a microwave field amplitude of 0.2 G and a magnetic field modulation amplitude of 0.4 G as calculated from cavity Q and peroxylamine disulfonate calibration (Fajer & Marsh, 1982). The spectrometer was equipped with a Bruker field-frequency lock to compensate for small frequency drifts. Temperature was controlled by flowing cooled N_2 gas through the radiation slits or by placing the cavity in a thermally insulated box. The spectra (100-G scan width, 4096 points) were acquired and averaged by using a Zenith 158 microcomputer (Zenith Data Systems, St. Joseph, MI) and a Data Translation 8021A A/D board (Data Translation Inc., Marlboro, MA) using software developed by the authors.
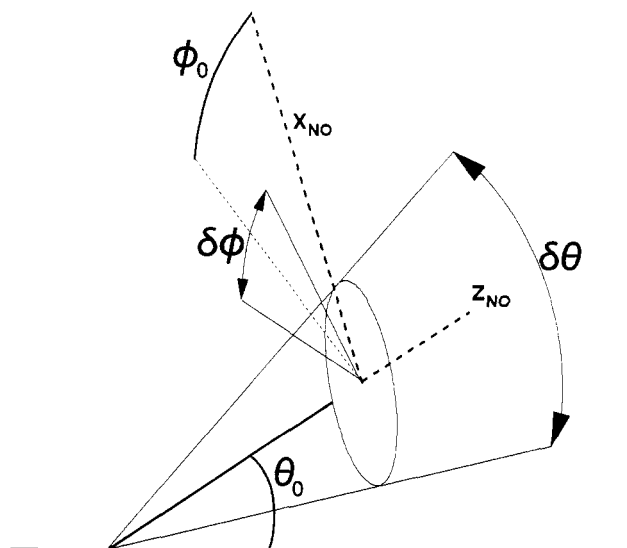

FIGURE 1: Definitions of the angles θ and ϕ, which define the orientation of the magnetic field **H** with respect to the principal axes of a nitroxide spin label when **H** is parallel to the fiber axis. These angles determine the orientational dependence of the EPR spectrum.

Experimental Protocol. To avoid possible artifacts associated with sample manipulation, the following protocol was carried out on each fiber bundle, without removing it from the EPR cavity: The spectrum was first recorded in rigor solution and then in ADP solution. Rigor was then restored by washing in rigor solution plus 3 mM EDTA, followed by rigor solution, and the spectrum was recorded again in rigor, to ensure that the structure and orientation of the fiber were not perturbed by washing and that no labeled S1 was washed out. Data were analyzed only if the initial and final rigor spectra were identical. The next wash was with 10 mM ascorbate, which reduced all the spins, and a base line was recorded. Finally, a solution of 0.2 mM peroxylamine disulfonate (PADS) was infused to determine the magnetic field center and range.

Data Processing. (a) Spectral Analysis. All spectra were recalculated according to the hyperfine splitting to and the position of the PADS spectrum by using software developed for this purpose. The PADS splitting was assumed to be 13.091 G and the center ($h\nu/g\beta$) assumed to correspond to a g value of 2.0056 (Faber & Fraenkel, 1973). The base-line spectrum was subtracted from the spectra in rigor and ADP, and the corrected spectra were then normalized to the same double-integrated intensity. The peak position was determined by least-squares fitting of second- and third-order polynomials to 0.5-G spectral windows. The base-line-crossing points were calculated by linear least-squares fits.

(b) Computer Fitting. The experimental spectra were condensed to 512 points, and simulations were fitted by using a simplex algorithm as described previously (Fajer et al., 1990). The myofibril spectra were fitted by simultaneous optimization of 11 tensor values and line-width parameters. Spectra of oriented fibers were simulated by assuming cylindrical symmetry with respect to the muscle fiber axis. The spin labels were assumed to have a Gaussian distribution of full width $\delta\theta$ about the average tilt angle θ_0 of the nitroxide spin label z axis $p(\theta) = \exp[-(\ln 2)\{(\theta - \theta_0)/\delta\theta/2\}^2]$. A similarly defined distribution was assumed for the twist angle ϕ (rotation of the x and y axes about the z axis, Figure 1). The total probability distribution is $p(\theta,\phi) = p(\theta)p(\phi)$, which is characterized by the four input parameters θ_0, ϕ_0, $\delta\theta$, and $\delta\phi$.

The four (for single Gaussian) or eight (for bimodal Gaussian) angular distribution parameters were optimized together with the magnetic parameters which were allowed

---

[2] Correction to Fajer et al. (1988) (printing error): concentration of Triton X-100 in fiber glycerinating buffer in Table I should be 0.5%.
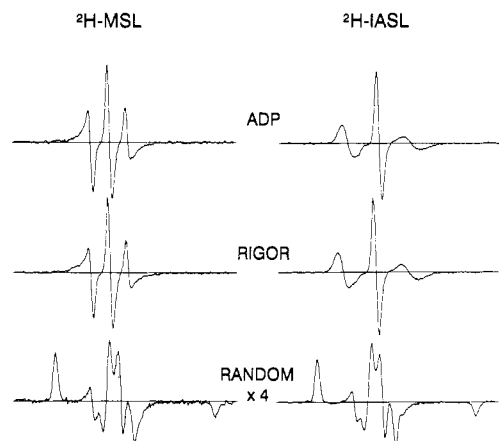
FIGURE 2: EPR spectra of muscle fibers decorated with ^{2}H-MSL-labeled (left) and ^{2}H-IASL-labeled (right) subfragment 1 (S1) at 23 °C, with fibers parallel to the magnetic field. (Top) ADP; (middle) rigor; (bottom) randomly oriented myofibrils in rigor.
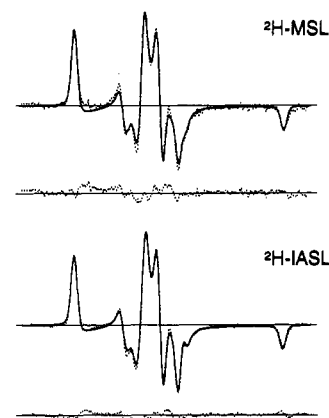

FIGURE 3: Fit of the myofibril spectra used to determine the orientation-independent tensor and line-width parameters in Table II. (Solid line) Computer fit; (dotted line) experimental spectra. The residual (the difference between the experimental spectrum and the fit) is shown below each spectrum.

to vary within the errors of myofibril fits. The details of simulations and of the fitting procedures are described in Fajer et al. (1990).

RESULTS

Experimental Spectra. EPR spectra of glycerinated fibers decorated with labeled S1 are shown in Figure 2 for ^{2}H-MSL and ^{2}H-IASL. When the fiber bundle is placed parallel to the magnetic field, the spectra in rigor and ADP exhibit three sharp lines, indicating a high degree of orientation (Figure 2) as originally found by Thomas and Cooke (1980) for protonated spin labels in rigor. The spectra of labeled S1 bound to myofibrils are typical of a randomly oriented sample, and they can be used to determine the intrinsic magnetic tensor and line-width values of the bound spin labels (Fajer et al., 1990).

The spectra in rigor and ADP are quite similar in appearance, and this is confirmed quantitatively by comparison of measured spectral parameters. The splitting between the outer lines for ^{2}H-MSL-S1 does not change by more than 0.1 G on addition of ADP. If we assume a single narrow Gaussian distribution of tilt angles θ, this implies that the mean tilt angle (θ_0, see Figure 1) does not change by more than 0.4° (Fajer et al., 1990). The position of the center line increases by 0.16 ± 0.05 G, indicating a change in the average twist (ϕ_0, see Figure 1) of 5 ± 2° (Fajer et al., 1990). There is also a significant difference in the width of the EPR lines. Closer inspection of the low-field region of the spectrum (Figure 2) reveals a shoulder in rigor that diminishes on addition of ADP (Figure 2). This is also borne out by a slight increase in the width of the high-field line in rigor, although a shoulder is not resolved. This subtle change is much more clear in these systems than in earlier studies with protonated spin labels, having a larger intrinsic line width. However, these results confirm our previous conclusion that the head does not rotate axially by more than 10° about any axis fixed within the head (Thomas et al., 1985).

For ^{2}H-IASL-S1, the effect of ADP is also quite small. The line splitting decreases by 1.0 ± 0.3 G, corresponding to an increase of 1.0 ± 0.3° in the average tilt angle θ_0. The position of the center of the spectrum does not change significantly, implying that the average twist angle ϕ_0 does not change by more than 0.4° upon ADP binding.

Determination of Angle-Independent Spectral Parameters. The accurate determination of the magnetic tensor values and line-width parameters is a prerequisite for high-resolution

determination of the angular distribution in oriented spectra (Fajer et al., 1990). The tensor and line-width values are most accurately determined by analyzing the spectrum from a randomly oriented sample, for which the spectrum is determined entirely by these parameters (Fajer et al., 1990). The spectra in Figure 3 were obtained from samples like those in Figure 2, except that the fibers were homogenized to produce myofibrils. The random orientation of these myofibrils was verified by reorienting the sample axis by 90° with respect to the magnetic field, producing an identical spectrum (data not shown).

Computer fitting of such spectra resulted in remarkably accurate reproduction of experimental line shapes (Figure 3). The values of all 11 magnetic parameters are given in Table I. The tensor and line-widths values in Table I were determined with surprising precision, often reaching that of the magnetic field inhomogeneity of 20 mG. The differences between the ^{2}H-MSL and ^{2}H-IASL values are due to the slightly different environment the two labels experience. At higher frequency (35 GHz) the fits were significantly improved by assuming an orientationally dependent Lorentzian line width (data not shown), but there was no significant effect at 9 GHz, so these corrections were neglected in further analyses.

Single-Gaussian Orientational Distribution. The spectra of labeled S1 bound to oriented fibers were first fitted by assuming a single orientational population with Gaussian distributions of the two angles (full width $\delta\theta$, $\delta\phi$), about the
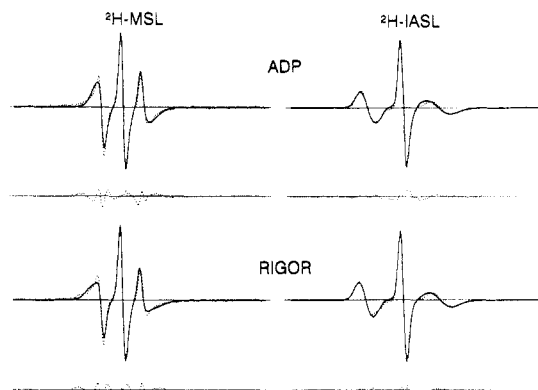
Table I: Magnetic Tensors and Line-Width Parameters[a]

parameter	^{2}H-MSL-S1	^{2}H-IASL-S1
g_x	2.009 050 ± 0.000 005	2.008 958 ± 0.000 002
g_y	2.006 106 ± 0.000 004	2.006 148 ± 0.000 002
g_z	2.002 406 ± 0.000 005	2.002 588 ± 0.000 002
T_x	7.41 ± 0.01	7.52 ± 0.01
T_y	7.63 ± 0.01	7.96 ± 0.01
T_z	35.39 ± 0.01	35.25 ± 0.05
Γ_L	0.55 ± 0.07	0.44 ± 0.01
$\Gamma_{L,\theta}$	0.22 ± 0.03	0.12 ± 0.01
$\Gamma_{L,\phi}$	0.15 ± 0.01	0.13 ± 0.01
Γ_G	1.63 ± 0.09	1.90 ± 0.01
Γ_{mG}	0.45 ± 0.11	0.54 ± 0.13

[a] g denotes the g tensor and T the hyperfine tensor. Γ_L and Γ_G are orientationally independent Lorentzian and Gaussian broadenings. $\Gamma_{L,\theta}$ and $\Gamma_{L,\phi}$ are the θ- and ϕ-dependent Lorentzians, and Γ_{mG} is the manifold-dependent Gaussian [see Fajer et al. (1990)]. T values and line widths in Gauss; g values are unitless. Errors are SEM of five searches.

FIGURE 4: Single-component fit to spectra of ^{2}H-MSL-labeled (left) and ^{2}H-IASL-labeled (right) S1 bound to oriented muscle fibers, used to obtain the orientational distribution in Figure 5. (Top) ADP; (bottom) rigor. The best-fit computer simulations (solid) are overlaid on experimental spectra (dotted). The residuals (experiment minus fit) are shown below the overlaid spectra.
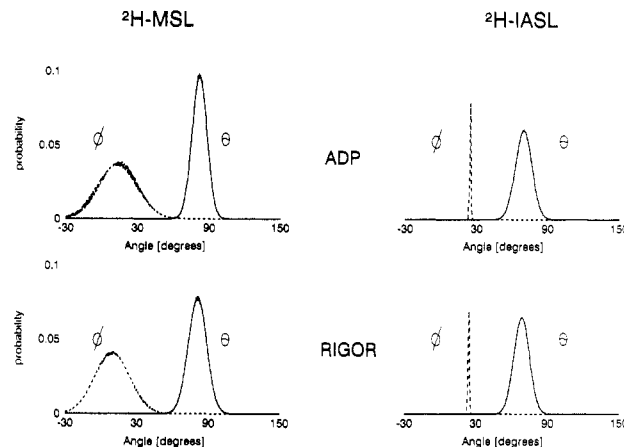

FIGURE 5: Single-Gaussian orientational distributions $\rho(\theta)$ and $\rho(\phi)$ resulting from the fits in Figure 4. (Top) ADP; (bottom) rigor. (Left) ^{2}H-MSL-S1; (right) ^{2}H-IASL-S1. For ^{2}H-IASL, $\rho(\phi)$ is divided by 10.

Table II: Single-Gaussian Distribution[a]

sample	θ_0	$\delta\theta$	ϕ_0	$\delta\phi$
^{2}H-MSL-S1				
ADP	82.04 ± 0.01	14.7 ± 0.2	13.6 ± 1.5	38.2 ± 1.2
rigor	80.83 ± 0.01	18.4 ± 0.3	9.4 ± 0.3	35.0 ± 0.8
^{2}H-IASL-S1				
ADP	69.69 ± 0.03	16.5 ± 0.1	24.8 ± 0.1	1.5 ± 0.3
rigor	68.40 ± 0.01	15.4 ± 0.1	24.1 ± 0.1	1.4 ± 0.1

[a] All values are in degrees. Errors are SEM of five successful searches.

average values (θ_0, ϕ_0). Computer fits shown in Figure 4 are adequate for ^{2}H-IASL-S1 but less so for ^{2}H-MSL-S1. In the latter case, inspection of the low-field part of the spectrum reveals poor reproduction of the shoulder mentioned above, and the residual reveals mismatch across the whole spectrum, indicating the presence of more than one Gaussian component (or a non-Gaussian distribution), both in rigor and in ADP. For ^{2}H-IASL-labeled S1, the residual is significantly smaller and is pronounced only in the center where the slope is steepest, magnifying any mismatch.

As seen in Figure 5 and Table II, the angular distribution for ^{2}H-MSL is similar in rigor and ADP. The value of the tilt angle θ_0 is about 80–82° with 14–18° disorder ($\delta\theta$). The twist angle ϕ_0 = 9–14° with 35–38° disorder ($\delta\phi$). In view of the rather poor fits to a single component, the values describing the single-Gaussian distribution in Table II might be misleading.

The angular distribution for ^{2}H-IASL is qualitatively different (Figure 5). In rigor, the tilt angle is centered about θ_0 = 68.4°, with a similar spread as for ^{2}H-MSL ($\delta\theta$ = 15.4°), the twist angle is centered about ϕ_0 = 24.1° with almost no disorder ($\delta\phi$ = 1.4°). The addition of ADP changes the distribution only very slightly: θ_0 increases by 1.3° and $\delta\theta$
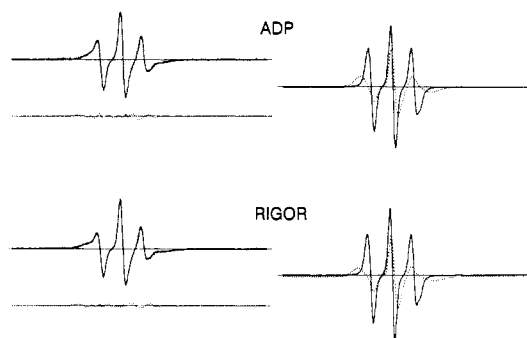

FIGURE 6: Two-component fit of the ^{2}H-MSL-S1 decorated fibers oriented parallel to the magnetic field. (Top) ADP; (bottom) rigor. (Left) Overlay of computer simulations and experimental spectra, with residuals shown below; (right) spectra corresponding to the two components of the simulated fit spectrum. The residuals are shown below the overlaid spectra.

decreases by 1° (Table II). ADP has an even smaller effect on the twist angle: ϕ_0 decreases by 0.7° without affecting $\delta\phi$.

Bimodal Gaussian Orientational Distribution. The fit to ^{2}H-MSL spectra is significantly improved when a linear combination of two spectra is assumed. The two spectral components are assumed to have the same magnetic tensors and line widths but different angular distributions. In the fitting of two components, the first one was limited to be within ±10° of values obtained from the single-component fit (Table II) on θ_0, ϕ_0, and $\delta\theta$, without restrictions on $\delta\phi$. On the basis of unrestricted, preliminary runs, θ_0 of the second component was restricted between 60° and 90°, without any assumptions about ϕ_0, $\delta\theta$, and $\delta\phi$ (Fajer et al., 1990). The resulting fits (Figure 6) are much improved over the single-component fits (Figure 4). The χ^2 value improves 3–5-fold, and the residuals are much smaller (Figures 4 and 6). ADP has very little effect on either component. In both ADP and rigor, the spectrum

Table III: Double-Gaussian Distribution[a]

sample	component A				component B				X_A
	θ_0	$\delta\theta$	ϕ_0	$\delta\phi$	θ_0	$\delta\theta$	ϕ_0	$\delta\phi$	
^{2}H-MSL-S1									
ADP	83.36 ± 0.32	7.3 ± 0.2	15.0 ± 0.5	12.2 ± 5.6	79.2 ± 1.6	21.3 ± 4.3	11.9 ± 2.7	51.1 ± 6.7	0.42 ± 0.04
rigor	83.55 ± 0.03	7.2 ± 0.1	12.3 ± 1.2	12.3 ± 1.2	75.9 ± 0.1	16.8 ± 0.3	13.6 ± 0.6	40.1 ± 1.6	0.41 ± 0.01
^{2}H-IASL-S1									
ADP	69.90 ± 0.02	15.2 ± 0.3	24.8 ± 0.2	1.6 ± 0.4	53.7 ± 4.3	53.5 ± 8.9	64.1 ± 13.8	39.8 ± 16.8	0.89 ± 0.02
rigor	68.43 ± 0.04	14.3 ± 0.2	23.8 ± 0.1	1.6 ± 0.3	53.0 ± 5.3	67.1 ± 1.5	48.2 ± 11.5	43.2 ± 17.6	0.92 ± 0.03

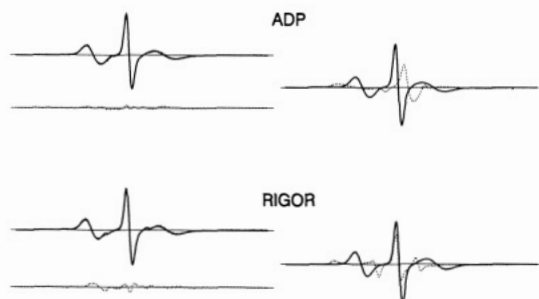[a] All values are in degrees. Errors are SEM of five successful searches.

FIGURE 7: Two-component fit of the ^{2}H-IASL-S1 decorated fibers parallel to the magnetic field. (Top) ADP; (bottom) rigor. (Left) Overlay of computer simulations and experimental spectra, with residuals shown below; (right) spectra corresponding to the two components of the simulated fit spectrum. The residuals are shown below the overlaid spectra.
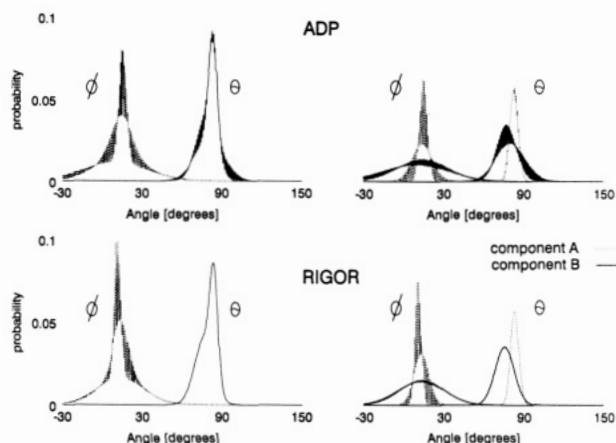

FIGURE 8: Double-Gaussian orientational distribution $\rho(\theta)$ and $\rho(\phi)$ resulting from the fits of Figure 6. Individual Gaussian components are shown on the right. (Top) ADP; (bottom) rigor. The thickness of the lines illustrates the uncertainty.

of the second component is slightly shifted downfield, has a larger splitting, and is much broader than that of the first component. Thus, the second component accounts for the shoulder in the low-field region of the rigor spectrum. Although the narrower component appears to dominate the spectrum, it only represents about 42% of the spin labels (Table III).

The inclusion of the second components in fitting ^{2}H-IASL spectra has a smaller effect than for ^{2}H-MSL (Figure 7). The improvement of χ^2 is 1.5–2-fold, and the second, broader component contributes no more than 10% of the intensity.

Figure 8 illustrates the two orientational components of ^{2}H-MSL. The components are of similar intensity and differ in θ_0 and the width of the distribution about θ_0 and ϕ_0. The second component is 3 times broader than the first, and its average tilt angle is shifted by 4–7°. The effect of ADP is mainly to increase ϕ_0 of the sharp component, change θ_0 and ϕ_0 of the broad component by less than 5°, and increase the spread of orientations by 5–11° (Table III).

Figure 9 illustrates the two-component orientational distribution obtained for ^{2}H-IASL. The small (10%) contribution of the second component did not affect the values obtained from the single-component analysis (Figure 9 and Table III). As before, ADP increased θ_0 by 1.5°, with a 0.9° increase in $\delta\theta$ of the principal component. The ϕ_0 changed by 1° without any change in the spread. Significantly, the minor component was also not much affected by ADP. The changes, if any, are at most 10° and are of the order of the errors in the determination of this small component.
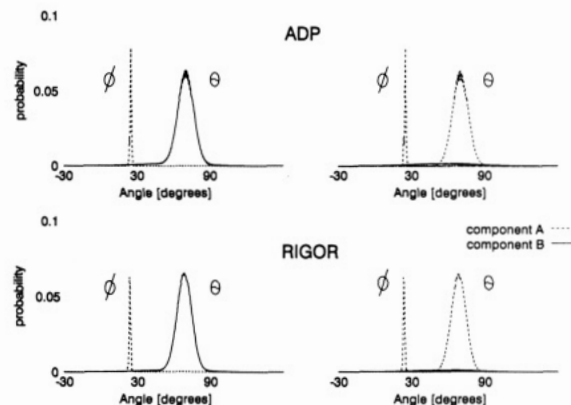

FIGURE 9: Double-Gaussian orientational distribution $\rho(\theta)$ and $\rho(\phi)$ resulting from the fits in Figure 7. Individual Gaussian components are shown on the right. (Top) ADP; (bottom) rigor. The thickness of the lines illustrates the uncertainty.

DISCUSSION

Summary of Results. In our previous preliminary paper on ADP effects on the orientation of standard protonated spin labels (Thomas et al., 1985), we concluded that no axis of the myosin head rotates by more than 10° due to ADP addition. In the present study, using deuterated spin labels to obtain higher resolution and using a quantitative method of spectral analysis to extract the maximum amount of information from the spectra, we confirm our earlier report for protonated maleimide spin label, extend it to a second spin label (^{2}H-IASL), and make it more quantitative. It is clear that ADP induces significant rotations of both IASL and MSL bound to myosin heads but that the rotations are very small, regardless of which spin label is used.

These conclusions do not depend on whether a single- or double-Gaussian distribution is assumed. For a single Gaussian (Table II), the ADP-induced change in average tilt angle (θ_0) of ^{2}H-MSL is 1.2° and the change in tilt disorder ($\delta\theta$) is 3.7°; the change in average twist angle (ϕ_0) is 4.2°, and the change in $\delta\phi$ is 3.2°. For ^{2}H-IASL, these changes are 1.3°, 1.1°, 0.7°, and 0.1°, respectively. The bimodal Gaussian analysis shows no rotation (change in θ_0 or ϕ_0) of major components by more than 5°, for either ^{2}H-MSL or ^{2}H-IASL. For both labels, the distribution of component B broadens slightly in the presence of ADP, but in no case does $\delta\theta$ or $\delta\phi$ increase by more than 5° in a major component. The larger changes in component B for ^{2}H-IASL should be ignored, since the molar fraction of this component is very small (<10%). The bimodal Gaussian model (Table III) improves the fits considerably for ^{2}H-MSL but not for ^{2}H-IASL, and the molar fractions are not the same for both spin labels, so there is no compelling evidence for two distinct orientational populations of the heads. Since IASL is known to react with cysteine 707 (SH1) more specifically than does MSL (Thomas et al., 1980), it is likely that the increased heterogeneity of the orientational distribution for ^{2}H-MSL is representative of labeling heterogeneity rather than head orientation. Thus, the ^{2}H-IASL distribution, which is nearly a single narrow Gaussian, probably reflects most accurately the distribution of head orientations. In any case, ADP does not affect the mole fraction X_A significantly, so there is no evidence from either label that ADP shifts the equilibrium between two orientational populations.

Relationship to Other Work. ADP is known to form a ternary complex with actin and myosin which most probably is part of the contractile cycle since it inhibits the maximum velocity of contraction (Cooke & Pate, 1985). Tanner et al. (1989) reported a 15% decrease in rigor tension in glycerinated

rabbit psoas fibers due to ADP, which was partially reversible upon ADP removal. ADP decreases the affinity of myosin for actin, possibly even detaching one head of the crossbridge at low protein concentrations, as suggested by proteolysis of acto–HMM complexes (Duong & Reisler, 1987; Chen & Reisler, 1984) and saturation-transfer EPR (Manuck et al., 1986).

Most fluorescence studies have also shown small or negligible effects of ADP on the orientation in rigor of probes attached to SH_1. The largest effect was observed for IATR, an iodoacetamido derivative of rhodamine (Borejdo, et al., 1982; Burghardt et al., 1983). The technique used (fluorescence detection of absorption dichroism) was capable of determining only one order parameter and thus could not provide detailed information about the orientational distribution of probes. Nevertheless, an upper bound of 22° was calculated for the rotation of rhodamine's absorption dipole relative to the fiber axis, assuming that most of the probes had no disorder and rotated from one discrete angle to another. Fluorescence anisotropy of IATR-labeled fibers was different in rigor and MgADP, but these changes were not quantified (Ajtai & Burghardt, 1986).

Another probe, IAEDANS, showed little or no change in fluorescence polarization due to ADP (Borejdo et al., 1982), but a later study of the wavelength dependence of fluorescence polarization did detect a small ADP effect (Ajtai & Burghardt, 1987). An analysis of the polarization change reveals no more than a 20° difference between the mean fluorophore emission dipole in rigor and in ADP, which is comparable to the resolution of the fluorescence technique (15–30°). Preliminary results quoted in the above work found no difference in the first four EPR order parameters in rigor and ADP.

However, in a more recent EPR work on protonated MSL-S1 (Ajtai et al., 1989) a significant difference in these order parameters was observed, suggesting a slight but significant reorientation of the protonated MSL spin label upon addition of MgADP. In agreement with the present study, the effect of ADP on the tilt angle β (θ) was barely observable, while larger effects were observed in the twist angle Γ (ϕ) in qualitative agreement with the present findings. There are some significant quantitative differences, notably the large negative probabilities for some orientations. The spectra of ^{1}H-MSL obtained by Ajtai et al. (1989) are very similar to spectra of ^{2}H-MSL in the present study, in that only very small spectral effects were observed upon ADP addition. Hence, the origin of different conclusions should be traced to the method of analyzing spectra. Our method, described in detail in Fajer et al. (1990), is a two-step simplex procedure. In the first step, the magnetic tensors and line widths are determined from the randomly oriented myofibril samples. In the second step, we fix these orientation-independent parameters and fit the experimental spectrum of an oriented fiber with the spectra representing single or bimodal Gaussian distributions. This sequential procedure eliminates much of the ambiguity in fitting, since variations in tensor values can have effects similar to variation in orientational parameters. The reliability of this method was extensively documented by fitting simulated spectra, comparing the original orientational distribution used for simulation with the distribution found by the fitting procedure (Fajer et al., 1990). The method used by Ajtai et al. (1989) analyzes only an oriented EPR spectrum, using a series expansion of the EPR spectrum without any a priori assumption about the functional form of the orientational distribution, allowing the orientation-independent parameters to vary freely with the orientational parameters. The reliability

of this method is not well documented, especially with respect to (a) retrieval of known orientational distributions from simulated spectra, (b) accuracy of the intrinsic magnetic parameters, which are not independently determined, and (c) the effect of noise present in experimental spectra. Moreover, the method employed by Ajtai et al. (1989) results in negative probabilities [Figure 2, Ajtai et al. (1989)]. This overshoot may be related to the Gibbs phenomenon, which is known to decrease the reliability and precision of functions represented by Fourier and related series (Arfken, 1970). We have found similar problems (e.g., negative probabilities) when testing this method on simulated EPR spectra with narrow orientational distributions.

The fluorescence and EPR studies discussed above have involved extrinsic probes attached covalently to the myosin head. Since it is conceivable that the probes modify myosin's response to ADP, it is important to examine ADP effects by using probes bound to sites other than SH_1 or to use intrinsic signals. A recent study of IANBD attached to SH_2 showed little or no change in orientation due to ADP (Ajtai & Burghardt, 1989). Polarization of intrinsic tryptophan fluorescence, which arises mainly from myosin heads, is sensitive to the transitions from rigor to relaxation and from relaxation to contraction, but not to the addition of MgADP in rigor (Aronson & Morales, 1969; dos Remedios et al., 1972). In summary, the orientations of most myosin-head-specific spectroscopic signals show little or no sensitivity to ADP addition, suggesting that the probes with the highest ADP sensitivity (IATR) do not reflect the global rotation of heads, but probably reflect local rotations of the probe or its immediate environment which seem to be not connected with force generation (Tanner et al., 1990). Another possibility, that a head rotates about the emission dipole of some fluorophores and about the z axis of spin labels, is ruled out by the present EPR results. Due to the 3D nature (nonaxial symmetry) of spin-label tensors, as contrasted with the 2D nature (axial symmetry) of optical chromophores, there is no orientation of the spin label that can make it insensitive to an axial head rotation of 1° or more.

These conclusions are supported by methods that are sensitive to global rotation rather than rotations of a localized probe. Birefringence is an intrinsic signal that is sensitive to myosin head orientation in fibers. This sensitivity to global reorientation makes it complementary to data from site-specific probes. The birefringence signal is sensitive to the transitions from rigor to relaxation and contraction, yet it is unaffected by MgADP (Oboriah & Irving, 1989). Low-angle X-ray diffraction, which is also sensitive to head orientation, showed no change when ADP was added to insect flight muscle in rigor, once again indicating that no large-scale axial or azimuthal rotations were induced (Rodger & Tregear, 1974).

The present study deals only with probes bound to labeled S1 diffused into fibers and bound to actin, but previous studies have consistently shown that the results are the same for labels bound to SH_1 on intrinsic heads in fibers, provided that the heads are bound to actin in both cases. This has been found in the absence of nucleotides (Borejdo et al., 1977; Thomas & Cooke, 1980) and in the presence of AMPPNP (Fajer et al., 1988) or pyrophosphate (Pate & Cooke, 1988). Finally, the lack of a large head rotation due to ADP does not imply that attached heads never rotate relative to actin, since we have shown previously that the attached heads execute microsecond motions in relaxed fibers at low ionic strength (Fajer et al., 1985) and in active fibers (Barnett & Thomas, 1989).

Conclusions. We have shown that ADP has a significant but very small effect on the orientation of bound myosin heads in decorated fibers. If this rotation is a part of the power stroke, then either (a) it is a very small fraction of the total power stroke or (b) the power stroke produces only a very small rotation of the labeled domain of myosin head. Future studies will extend this work to labels attached to intrinsic heads in muscle fibers and apply this method of analysis to other states in the contractile cycle.

REFERENCES

Ajtai, K., & Burghardt, T. P. (1986) *Biochemistry 25*, 6203–7.

Ajtai, K., & Burghardt, T. P. (1987) *Biochemistry 26*, 4517–23.

Ajtai, K., & Burghardt, T. P. (1989) *Biochemistry 28*, 2204–10.

Ajtai, K., French, A. R., & Burghardt, T. P. (1989) *Biophys. J., 56*, 535–541.

Arfken, G. (1970) in *Mathematical Methods for Physicists*, pp 665–666, Academic Press, New York.

Aronson, J. F., & Morales, M. F. (1969) *Biochemistry 8*, 4517–4522.

Barnett, V. A., & Thomas, D. D. (1989) *Biophys. J. 56*, 517–523.

Borejdo, J., & Putnam, S. (1977) *Biochim. Biophys. Acta 459*, 578–95.

Borejdo, J., Assulin, O., Ando, T., & Putnam, S. (1982) *J. Mol. Biol. 158*, 391–414.

Burghardt, T. P., & Ajtai, K. (1985) *Proc. Natl. Acad. Sci. U.S.A. 82*, 8478–82.

Burghardt, T. P., & Ajtai, K. (1989) *Proc. Natl. Acad. Sci. U.S.A. 86*, 5366–70.

Burghardt, T. P., Ando, T., & Borejdo, J. (1983) *Proc. Natl. Acad. Sci. U.S.A. 80*, 7515–9.

Chen, T., & Reisler, E. (1984) *Biochemistry 23*, 2400–7.

Cooke, R. (1986) *CRC Crit. Rev. Biochem. 21*, 53–118.

Cooke, R., & Pate, E. (1985) *Biophys. J. 48*, 789–98.

Cooke, R., Crowder, M. S., Wendt, C. H., Barnett, V. A., & Thomas, D. D. (1984) *Adv. Exp. Med. Biol., 170*, 413–27.

Dos Remedios, C. G., Yount, R. G., & Morales, M. F. (1972) *Proc. Natl. Acad. Sci. U.S.A. 69*, 2542–6.

Duong, A. M., & Reisler, E. (1989) *Biochemistry 28*, 1307–13.

Faber, J. J., & Fraenkel, G. K. (1967) *J. Chem. Phys. 47*, 2462–67.

Fajer, P. G., & Marsh, D. (1982) *J. Magn. Reson. 49*, 212–224.

Fajer, P. G., Fajer, E. A., Svensson, E., Brunsvold, N., Wendt, C., & Thomas, D. D. (1985) *Biophys. J. 47*, 380a.

Fajer, P. G., Fajer, E. A., Brunsvold, N. J., & Thomas, D. D. (1988) *Biophys. J. 53*, 513–24.

Fajer, P. G., Bennett, R., Polnaszek, C. F., Fajer, E. A., Thomas, D. D. (1990) *J. Magn. Reson. 88*, 111–125.

Huxley, H. E. (1969) *Science 164*, 1356–65.

Manuck, B. A., Seidel, J. C., & Gergely, J. (1986) *Biophys. J. 50*, 221–30.

Mendelson, R. A., & Wilson, M. G. (1982) *Biophys. J., 39*, 221–7.

Morales, M. F., & Botts, J. (1979) *Proc. Natl. Acad. Sci. U.S.A. 76*, 3857–9.

Oboriah, O., & Irving, M. (1989) *Biophys. J. 55*, 9a.

Pate, E., & Cooke, R. (1988) *Biophys. J. 53*, 561–73.

Rodger, C. D., & Tregear, R. T. (1974) *J. Mol. Biol. 86*, 495–7.

Siemankowski, R. F., & White, H. D. (1984) *J. Biol. Chem. 259*, 5045–53.

Tanner, J. W., Vallette, D. P., Thomas, D. D., & Goldman, Y. E. (1989) *Biophys. J. 55*, 9a.

Tanner, J. W., Thomas, D. D., & Goldman, Y. E. (1990) *Biophys. J. 57*, 398a.

Thomas, D. D. (1987) *Annu. Rev. Physiol. 49*, 691–709.

Thomas, D. D., & Cooke, R. (1980) *Biophys. J. 32*, 891–906.

Thomas, D. D., Seidel, J. C., Hyde, J. S., & Gergely, J. (1975) *Proc. Natl. Acad. Sci. U.S.A. 72*, 1729–33.

Thomas, D. D., Svensson, E., & Polnaszek, C. (1985) *Biophys. J. 47*, 380a.

Yanagida, T. (1981) *J. Mol. Biol. 146*, 539–60.